Research Article

Annals of Civil Engineering and Management

Enhanced Electrochemical Performance of $FeCo_2S_4$@g-C_3N_4 Composites for Advanced Energy Storage Applications

Shahadat Ali[1*], Tahreem Shahzad[2] and Mujahid Hussain[3]

[1]*Center of Excellence in Solid State Physics, University of The Punjab, Pakistan*

[2]*Department of Chemistry, University of Narowal, Pakistan*

[3]*Department of Chemistry, University of Okara, Pakistan*

[*]Corresponding Author
Shahadat Ali,Center of Excellence in Solid State Physics, University of The Punjab, Pakistan.

Submitted: 2024, Oct 18; **Accepted:** 2024, Nov 15; **Published:** 2024, Nov 22

Citation: Ali, S., Shahzad, T., Hussain, M. (2024). Enhanced Electrochemical Performance of $FeCo_2S_4$@g-C_3N_4 Composites for Advanced Energy Storage Applications. *Ann Civ EngManag, 1*(1), 01-08.

Abstract

At present, the world faces an unprecedented challenge regarding energy issues. To tackle these issues, there is a growing focus on the advancement of advanced energy storage solutions. This study explores the potential of newly developed nanostructures (NSs) made of iron cobalt sulfide-graphitic carbon nitride ($FeCo_2S_4$@g-C_3N_4) for innovative applications in supercapacitors. The necessary materials were synthesized through the hydrothermal method, ensuring a robust nanostructure foundation. The successful creation of the composite NSs was confirmed through XRD and EDX analysis, verifying both phase purity and compositional consistency. SEM revealed a variety of morphologies, with a unique combination of spherical nanoparticles and sheet-like structures that maximize surface area for enhanced electrochemical interactions. The $FeCo_2S_4$@g-C_3N_4 NS electrode demonstrated impressive electrochemical performance, demonstrating a specific capacitance of 2460 Fg^{-1} at 1.5 Ag^{-1}, an energy density of 85.4 $Whkg^{-1}$, and a power density of 375 Wkg^{-1}. This investigation underscores the promise of $FeCo_2S_4$@g-C_3N_4 NS for advanced energy storage solutions, potentially paving the way for next-generation supercapacitors with high energy and power outputs.

Keywords: Electrochemical Properties, Nanocomposites, Energy Storage, Iron-Cobalt Sulfide, Graphitic Carbon Nitride

1. Introduction

Recently, the demand for energy has surged due to population growth and advancements in commercial and industrial sectors. Meeting this demand, given the depletion of fossil fuel resources, has led to the adoption of renewable energy sources such as solar and wind, which emphasize the need for efficient energy storage devices to manage their intermittent nature [1-3]. Supercapacitors have appeared as promising solutions in this regard, offering high-power output, rapid charge-discharge capabilities, and excellent cycling stability compared to traditional energy storage devices [4-7]. However, supercapacitors' energy density is limited by their charge storage mechanisms, which involve either EDLCs or pseudo capacitors. EDLCs store charge electrostatically at the electrode-electrolyte interface, delivering high power but lower energy density, while pseudo-capacitors achieve higher energy storage through rapid and reversible redox reactions [8,9].Research to improve supercapacitor energy density without forgoing power density has focused on developing nanostructured composite electrode materials. These composites integrate electrochemically active components with highly conductive carbon-based materials, such as graphene, to achieve enhanced performance [10-13]. Graphene's high surface area, mechanical robustness, and excellent conductivity make it an ideal material for energy storage applications, especially when used in composite forms that combine multiple beneficial properties. Among electrode materials, transition metal sulfides, especially those based on iron, show great potential due to their complex redox processes and improved intrinsic conductivity over metal oxides [14-16].Ternary iron compounds, particularly iron cobalt sulfide ($FeCo_2S_4$), offer additional benefits due to structural flexibility and the synergistic electrochemical activity of multiple metal ions [17,18].

$FeCo_2S_4$ has demonstrated impressive pseudocapacitive performance, but it also faces challenges such as lower ion and electron mobility, limited conductivity, and potential structural degradation during cycling, which can affect its rate capability and cycle stability [19-21]. Integrating $FeCo_2S_4$ with conductive carbon-based materials like graphitic carbon nitride (g-C_3N_4)

may overcome these limitations by combining the fast electron transport capabilities of g-C_3N_4 with the redox charge storage properties of $FeCo_2S_4$ [22-25].The $FeCo_2S_4$@g-C_3N_4 composite remains relatively unexplored in the context of electrochemical energy storage. This study introduces a hydrothermal synthesis method to produce $FeCo_2S_4$@g-C_3N_4 nanostructures for use as electrode materials in high-efficiency supercapacitors. The composite's hierarchical, porous architecture enhances electron mobility, promotes rapid ion diffusion, and provides numerous active sites. Electrochemical properties of the $FeCo_2S_4$@g-C_3N_4 electrodes were examined using a three-electrode system in a 2M KOH aqueous solution. The optimized electrode, composed of 50% $FeCo_2S_4$ and 25% g-C_3N_4, delivered an impressive specific capacitance of 2210.2 F/g at a 1 mV/s scan rate, alongside high energy and power densities of 85.4 Wh/kg and 375 W/kg, respectively.The paper is structured to comprehensively detail the study of $FeCo_2S_4$@g-C_3N_4 composites as potential electrode materials.

The Abstract provides a concise summary of the research objectives, methods, and findings. The Introduction covers the background and significance of advanced energy storage materials, emphasizing the potential of supercapacitors. The Experimental Section outlines the materials used, the synthesis processes for $FeCo_2S_4$ and g-C_3N_4, and the techniques applied for characterization. In the Results and Discussion, detailed analyses are presented: EDX for composition, XRD for crystal structure, SEM for morphology, CV, and GCD for electrochemical performance, and EIS for conductivity and resistance insights. Finally, the Article Type: Reviewhighlights the key findings, proposing $FeCo_2S_4$@g-C_3N_4 as a promising material for supercapacitor applications.

2. Experimental

2.1. Materials

The $FeCo_2S_4$@g-C_3N_4 precursor was sourced from Sigma-Aldrich, classified as analytical grade, and comprised cobalt (II) nitrate hexahydrate ($Co(NO3)_2 \cdot 6H_2O$), thioacetamide (CH_3CSNH_2), sodium hydroxide (NaOH), melamine ($C_3H_6N_6$), and iron (II) nitrate hexahydrate ($Ni(NO_3)_2 \cdot 6H_2O$). These chemicals were utilized in the experiments without any additional purification steps. To maintain the purity of the materials throughout the procedures, deionized water was used exclusively.

2.2. Synthesis of $FeCo_2S_4$

$FeCo_2S_4$ nanoparticles were synthesized using a low-temperature, cost-efficient hydrothermal method. Initially, 0.5 mmol of $Fe(NO_3)_2 \cdot 6H_2O$ and 1 mmol of $Co(NO_3)_2 \cdot 6H_2O$ were dissolved in deionized water on a magnetic stirrer for 20 minutes, resulting in a purple solution. To accelerate the reaction and ensure purity, 5 mmol of NaOH and 4 mmol thioacetamide (TAA)in the solution were added gradually. The mixture was then stirred gently for an additional 30 minutes to promote thorough integration. Following this, the solution was pouredinto a 100 mL autoclave and heated to 200 °C in an oven, as illustrated in Figure 1(a). This controlled environment was maintained for 12 hours, facilitating the synthesis of $FeCo_2S_4$ nanoparticles.The synthesized $FeCo_2S_4$ nanoparticles underwent extensive purification through several centrifugation cycles, aimed at enhancing the quality of the final product by eliminating any potential impurities. Subsequently, the purified $FeCo_2S_4$ nanoparticles were dried at 60 °C for several hours to remove any residual moisture.

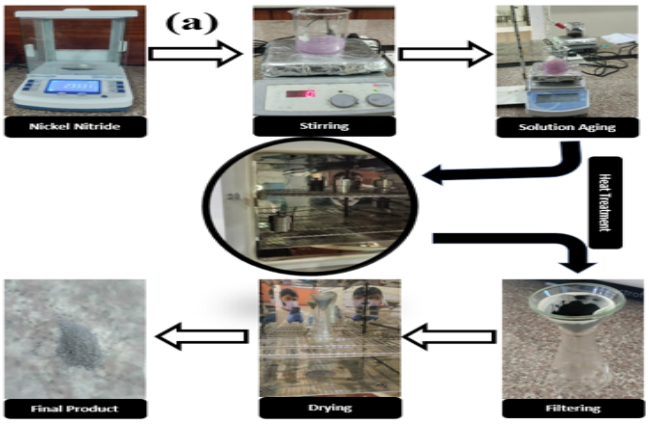

Figure 1(a): Schematic Synthesis of $NiCo_2S_4$

2.3. Synthesis of g-C_3N_4

To synthesize g-C_3N_4, a straightforward thermal decomposition technique was applied using melamine at a temperature of 550 °C. In this procedure, 50 grams of melamine were placed into an alumina crucible and heated in a muffle furnace. The temperature was increased at a steady rate of 5 °C per minute until reaching 550 °C, as depicted in Figure 1(b). The sample was maintained at this temperature for 180 minutes, after which the crucible was allowed to cool to room temperature. Once cooled, the resulting g-C_3N_4 powder displayed a characteristic yellow color. This approach provides an effective and simple method for generating g-C_3N_4 via melamine decomposition.

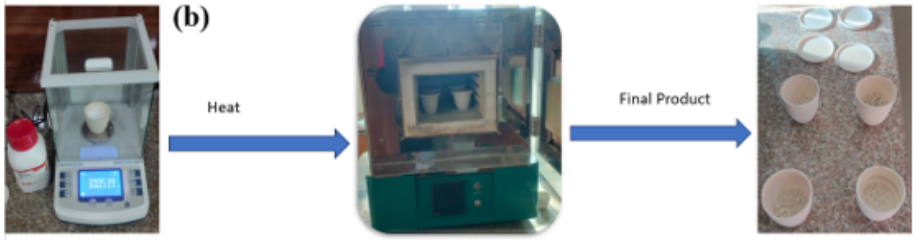

Figure 1(b): Schematic Synthesis of g-C_3N_4

2.4. Composite Preparation of $FeCo_2S_4$@g-C_3N_4

The composites were fabricated by varying the weight percentages of $FeCo_2S_4$ and g-C_3N_4 in a 50:50 ratio, utilizing the solid-state technique. During this procedure, a mortar and pestle were employed to create a uniform mixture of the materials, ensuring homogeneity throughout the composite.

2.4.1. Characterizations

The crystal structures of $FeCo_2S_4$@g-C_3N_4 nanocomposites were inspected using X-ray diffraction (XRD) analysis. Data collection was conducted utilizing a Tongda TD-3500 diffractometer, which was equipped with CuKα radiation (λ = 1.5418 Å) and scanned across a 2θ range from 10° to 90°. To examine the morphology of the synthesized electrode materials, an MIRA3 TESCAN SEM was utilized with a 5.0 kV accelerating voltage. Elemental composition was further analyzed by coupling the SEM with EDX. Additionally, various electrochemical properties were assessed with a GAMRY Reference 5000 (14543) electrochemical workstation.

3. Results and Discussions

3.1. EDX

The EDX method was applied to evaluate the chemical compositions of $FeCo_2S_4$ and $FeCo_2S_4$@g-C_3N_4 nanostructures. As demonstrated in Figure2a, the EDX spectra of $FeCo_2S_4$ mainly indicate the presence of iron, cobalt, and sulfur. In the EDX spectra of Ni2CoS4@g-C_3N_4 (Figure2b), in addition to iron, cobalt, and sulfur, carbon, and nitrogen, were identified, showing the effective hydrothermal stabilization of metal-sulfide NSs on the g-C_3N_4 surface. These results indicate the successful production of both g-C_3N_4 and $FeCo_2S_4$@g-C_3N_4 nanostructures.

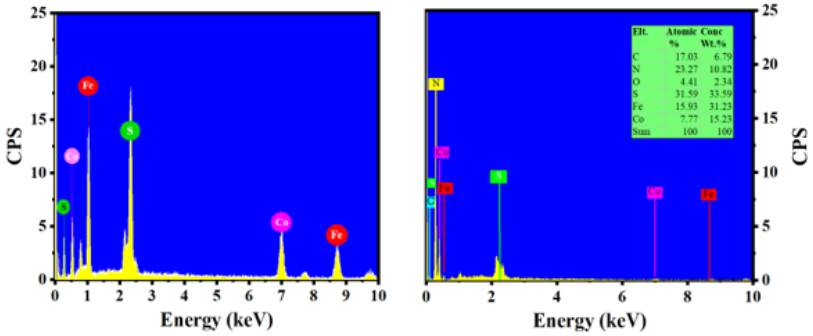

Figure 2: EDX of (a) $FeCo_2S_4$ (b) $FeCo_2S_4$@ g-C_3N_4

3.2. XRD

XRD analysis was performed to investigate the crystalline structures of the synthesized nanostructures. Figure 3(a, b) displays the XRD patterns for $FeCo_2S_4$@g-C_3N_4 and pure g-C_3N_4. Both samples exhibit characteristic peaks of g-C_3N_4 at 13.25° (100) and 27.10° (101), aligning well with previously reported values in the literature[26]. The peak at 13.25° is associated with the in-plane structural arrangement of tri-s-triazine units, while the peak at 27.10° corresponds to the interlayer stacking typically seen in conjugated aromatic systems.

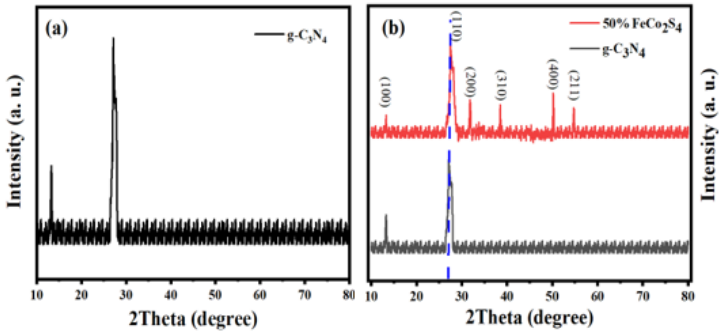

Figure 3: XRD Pattern of (a) g-C_3N_4 (b) $FeCo_2S_4$@g-C_3N_4

The XRD pattern of $FeCo_2S_4$@g-C_3N_4 reveals cubic characteristic peaks ofFeCo2S4 (JCPDS No. 24-0334) at 2theta values of 27.5° (110), 31.8° (200), 38.5° (310), 50.2° (400), and 54.7° (211), alongside those of g-C_3N_4. This confirms the successful incorporation of $FeCo_2S_4$ nanoparticles into the g-C_3N_4 matrix.

3.3. SEM

The SEM pictures of the $FeCo_2S_4$@g-C_3N_4 composite at various magnifications indicate a homogeneous dispersion of $FeCo_2S_4$ nanoparticles throughout the g-C_3N_4 layered structure. At reduced magnification (left), the composite displays well-dispersed $FeCo_2S_4$ particles covering the g-C_3N_4 surface, giving many active sites that are beneficial for redox reactions. At increased magnification (right), the nanoparticles are shown to be strongly fixed to the g-C_3N_4 layers, promoting efficient electron transport and structural integrity.

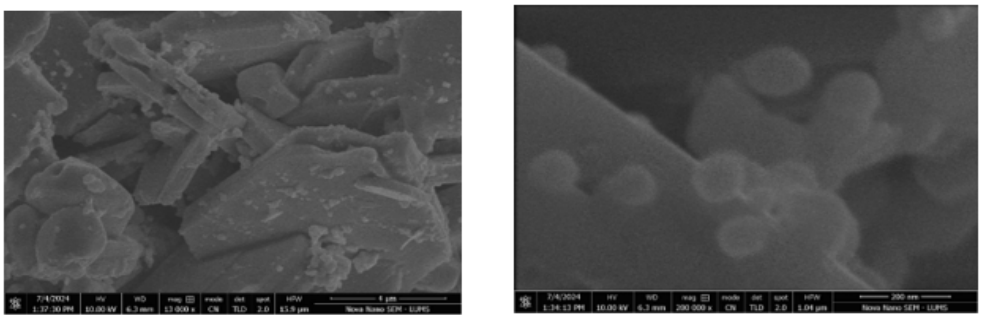

Figure 4: SEM Images of $FeCo_2S_4$@g-C_3N_4 at Different Magnifications

3.4. CV

CV was performed at a sweep rate of 50 mV/s to examine the electrochemical properties of the synthesized electrode materials. The voltammograms for g-C_3N_4 and $FeCo_2S_4$ reveal redox peaks corresponding to the Fe^{2+}/Fe^{3+} and Co^{2+}/Co^{3+} transitions, indicating reversible redox reactions. These peaks are associated with the insertion and extraction of OH^- anions during the CV measurements, reflecting the materials' charge storage behavior[27].

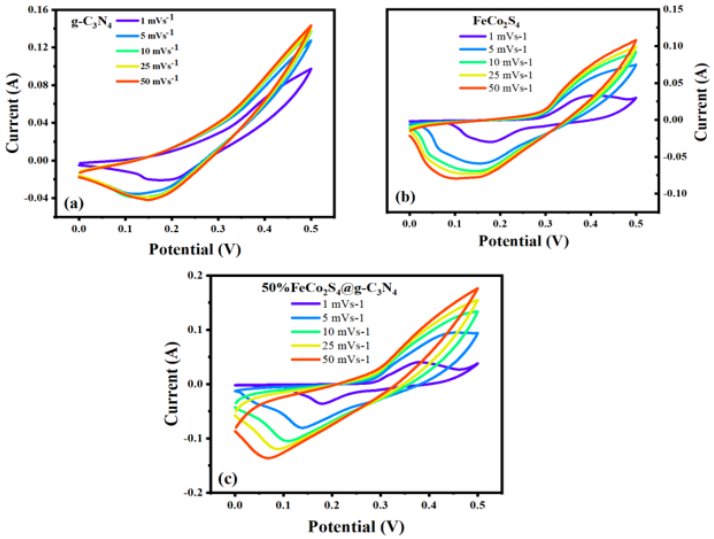

Figure 5: CV Graphs at Different Scan Rates of (a) g-C_3N_4 (b) $FeCo_2S_4$ (c) $FeCo_2S_4$@g-C_3N_4

The specific capacitance (Cs) can be expressed as:

$$Cs = \frac{\int IdV}{2 \times m \times v \times \Delta V}$$

where IdV represents the integral of the area under the voltammogram curve, mmm is the mass of the NS, ΔV is the voltage, and v is the potential rate.

The $FeCo_2S_4$@g-C_3N_4 composite exhibited significantly improved electrochemical performance compared to both g-C_3N_4 nanosheets and $FeCo_2S_4$ nanoparticles. This enhancement can be attributed to the synergistic interaction between iron and cobalt sulfides within the $FeCo_2S_4$@g-C_3N_4 composite. The large surface area of g-C_3N_4 offers abundant sites for the deposition of iron and/or cobalt sulfide nanoparticles, providing an increased number of active sites for OH^- ion absorption and release, outperforming unsupported $FeCo_2S_4$ nanoparticles.

CV was recorded for the proposed electrode materials at different scan rates, as shown in Figure 5(a-c). The 50% $FeCo_2S_4$@g-

C_3N_4 composite maintained a superior rate capability across scan rates from 1 mV/s to 50 mV/s, even though both materials showed a decrease in specific capacitance with higher scan rates due to diffusion limitations. This enhanced rate capability is due to the larger surface area of g-C_3N_4, which increases active sites for $FeCo_2S_4$ nanoparticle deposition, facilitating charge and ion transport between the electrode material and the electrolyte.

Electrode	50	25	10	5	1
	mVs^{-1}	mVs^{-1}	mVs^{-1}	mVs^{-1}	mVs^{-1}
	(Fg^{-1})	(Fg^{-1})	(Fg^{-1})	(Fg^{-1})	(Fg^{-1})
50% $FeCo_2S_4$	155.46	203.35	311.12	526.79	2210.2
$FeCo_2S_4$	82.87	128.03	178.64	319.35	1502.58
g-C_3N_4	23.19	76.62	152.63	219.03	795.46

Table 1: Cs Values of Fabricated Electrodes at Different Scan Rates

3.5. GCD

The GCD curves highlight the excellent electrochemical properties of the fabricated electrode samples across different current densities (1.5 A/g, 2 A/g, and 2.5 A/g) within a potential window of 0.0 to 0.5 V in a 2 M KOH alkaline solution (Figure 6). The nonlinearity observed in the GCD curves indicates a pseudocapacitive charge storage mechanism, which is crucial for understanding the charge storage characteristics of these materials.

The specific capacitance (Cp), the energy density (Ed), and the power density (Pd) are calculated using the following equations:

C_p:

$$Cp = \frac{I \times \Delta t}{\Delta V \times m}$$

E_d:

$$Ed = \frac{Cp \times (\Delta v)^2}{2 \times 3.6}$$

P_d:

$$Pd = \frac{Ed \times 3600}{\Delta t}$$

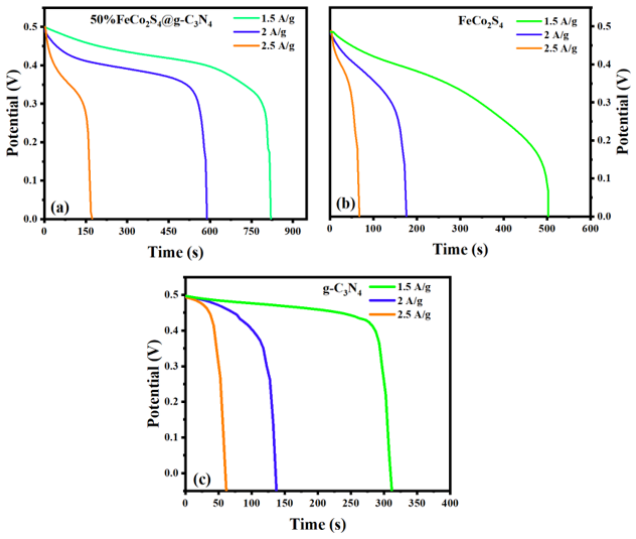

Figure 6: GCD Graphs at Different Scan Rates of (a) g-C_3N_4 (b) $FeCo_2S_4$ (c) $FeCo_2S_4$@g-C_3N_4

Here, I represent the current (A), Δt is the discharging time (s), m is the active mass (g), and ΔV is the potential window[28].The 50%$FeCo_2S_4$/g-C_3N_4 nanocomposite's GCD curves showed longer discharging times than those of the pure g-C_3N_4 and $FeCo_2S_4$ nanocomposites among the investigated samples. The (50%) $FeCo_2S_4$@(50%) g-C_3N_4 nanocomposite's larger surface area offers additional ion storage locations during charging, which increases capacitance. The specific capacitance value of 2210 F/g derived from the CV curves nearly matched the peak specific capacitance of 2460 F/g obtained from the GCD plot at 1.5 A/g. Furthermore, 375 W/kg and 85.4 Wh/kg, respectively, were measured for the appropriate power density and energy density.The total capacitance measurement is reduced as a consequence of this restriction. The Cp derived from the GCD curves is summarized in Table 2.

3.6. EIS

As seen in Figure 7(a-d), the conductivity and internal resistance of the synthesized materials, such as pure g-C_3N_4, $FeCo_2S_4$ NSs, and 50% $FeCo_2S_4$@g-C_3N_4 nanocomposites, were examined using EIS analysis. Three different zones may be distinguished from the frequency range of 0.1 KHz to 100 KHz across which EIS measurements were made: Charge transfer resistance is shown by

the semicircle's diameter. In the high-frequency range, internal resistance is shown. Ion diffusion resistance is represented by the low-frequency zone's straight line.The narrow semicircle seen in the high-frequency band indicates that the optimized sample has minimal internal resistance [29-31]. The combination of synthesized materials, which included 50% $FeCo_2S_4$@g-C_3N_4 nanocomposites, pure g-C_3N_4, and pure $FeCo_2S_4$ NSs, showed promising metallic conductive properties as electrode materials for supercapacitors.

Electrode Material	Current Density (A/g)	Discharge Time (s)	Potential Window (V)	Specific Capacitance (Fg-1)	Energy Density (Wh/Kg)	Power Density (W/Kg)
50% FeCo2S4@g-C3N4	1.5	820	0.5	2460	85.417	375
	2	590	0.5	2360	81.944	500
	2.5	170	0.5	850	29.514	625
FeCo2S4	1.5	510	0.5	1530	53.125	375
	2	176	0.5	704	24.444	500
	2.5	68	0.5	340	11.806	625
g-C3N4	1.5	310	0.5	930	32.292	375
	2	135	0.5	540	18.750	500
	2.5	60	0.5	300	10.417	625

Table 2: The Specific Capacitance, Power Density, and Energy Density of All Three Fabricated Electrodes at Different Current Densities

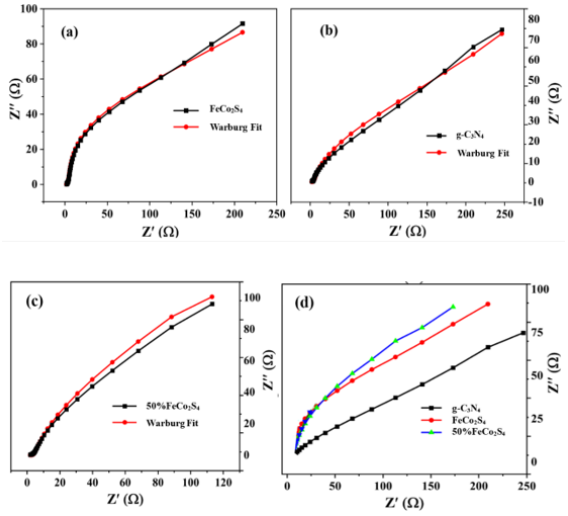

Figure 7(a-d): Nyquist Plots of(a) g-C_3N_4 (b) $FeCo_2S_4$ (c) $FeCo_2S_4$@g-C_3N_4 (a) Combine

The uncompensated resistance (Ru) of the 50% $FeCo_2S_4$@g-C_3N_4 nanocomposite electrode was determined to be 1.533 Ω, which is less than the resistance of the pure FeCo2S4electrode at 2.589 Ω. Additionally, the electrical conductivity of the 50% $FeCo_2S_4$@g-C_3N_4 nanocomposite was found to be higher than that of $FeCo_2S_4$ NSs. The charge transfer resistance (Rct) values for g-C_3N_4, $FeCo_2S_4$ NSs, and 50% $FeCo_2S_4$@g-C_3N_4 nanocomposites were calculated to be 0.00573, 0.00483, and 0.00156 Ω, respectively. According to the EIS spectra, pure g-C_3N_4 NSs have a higher percentage of pure $FeCo_2S_4$ NSs at lower frequencies, which is associated with a lower diffusion ion resistance. The low-frequency domain of a perfect supercapacitor should display a straight line parallel to the imaginary axis. With an increase in the ratio of pure $FeCo_2S_4$ NSs, the slope and supercapacitive behavior of the 50% $FeCo_2S_4$@g-C_3N_4 nanocomposite are enhanced. This indicates the improved electrochemical performance and potential applicability of these nanocomposite materials in energy storage systems.

4. Conclusion

For energy storage applications, a new electrode material has been created with an emphasis on different iron and/or cobalt sulfide nanoparticles supported on g-C_3N_4 nanosheets. A variety of spectroscopic and electrochemical methods were used to characterize the synthesized nanostructures, and the results showed that the $FeCo_2S_4$@g-C_3N_4 composite performed the best out of all the nanostructures that were evaluated. It demonstrated superior energy storage capacity, high coulombic efficiency, prolonged cyclic life, and impressive rate capability. These findings suggest that the $FeCo_2S_4$@g-C_3N_4 nanostructure could serve as an effective electrode material for advanced energy storage devices, potentially contributing to the development of more efficient and reliable energy systems. This recommendation aligns with recent trends in

nanomaterials for energy applications, emphasizing the importance of composite materials that enhance performance metrics ding on the subject, you can check out sources that discuss recent advancements in energy storage materials and their applications.

References

1. Varghese, S. (2023). Future of Energy. *Future Intelligence*, 53.
2. Armstrong, R., Chiang, Y. M., Gruenspecht, H., Brushett, F., Deutch, J., Engelkemier, S., ... &Mallapragada, D. (2022). The future of energy storage. *Massachusetts Institute of Technology, Cambridge, MA.*
3. Ives, M., Righetti, L., Schiele, J., De Meyer, K., Hubble-Rose, L., Teng, F., ... & Hepburn, C. (2021). A new perspective on decarbonising the global energy system
4. Zhang, L. L., & Zhao, X. S. (2009). Carbon-based materials as supercapacitor electrodes. *Chemical society reviews, 38*(9), 2520-2531.
5. Conway, B. E. (2013). *Electrochemical supercapacitors: scientific fundamentals and technological applications. Springer Science & Business Media.*
6. Simon, P., &Gogotsi, Y. (2008). Materials for electrochemical capacitors. Nature materials, 7(11), 845-854.
7. Sharma, P., & Kumar, V. (2020). Current technology of supercapacitors: A review. *Journal of Electronic Materials, 49*(6), 3520-3532.
8. Chodankar, N. R., Pham, H. D., Nanjundan, A. K., Fernando, J. F., Jayaramulu, K., Golberg, D., ... &Dubal, D. P. (2020). True meaning of pseudocapacitors and their performance metrics: asymmetric versus hybrid supercapacitors. *Small, 16*(37), 2002806.
9. Ashritha, M. G., &Hareesh, K. (2023). Electrode materials for EDLC and pseudocapacitors. *In Smart Supercapacitors* (pp. 179-198). Elsevier.
10. Bose, S., Kuila, T., Mishra, A. K., Rajasekar, R., Kim, N. H., & Lee, J. H. (2012). Carbon-based nanostructured materials and their composites as supercapacitor electrodes. *Journal of Materials Chemistry, 22*(3), 767-784.
11. Liu, L., Niu, Z., Zhang, L., Zhou, W., Chen, X., &Xie, S. (2014). Nanostructured graphene composite papers for highly flexible and foldable supercapacitors. *Advanced Materials, 26*(28), 4855-4862.
12. Li, J., Yang, Q., &Zhitomirsky, I. (2010). Composite electrodes for electrochemical supercapacitors. *Nanoscale research letters, 5,* 512-517.
13. Jiang, J., Zhang, Y., Nie, P., Xu, G., Shi, M., Wang, J., ... & Zhang, X. (2018). Progress of nanostructured electrode materials for supercapacitors. *Advanced Sustainable Systems, 2*(1), 1700110.
14. Mao, S., Lu, G., & Chen, J. (2015). Three-dimensional graphene-based composites for energy applications. *Nanoscale, 7*(16), 6924-6943.
15. Pothu, R., Bolagam, R., Wang, Q. H., Ni, W., Cai, J. F., Peng, X. X., ... & Ma, J. M. (2021). Nickel sulfide-based energy storage materials for high-performance electrochemical capacitors. *Rare Metals, 40,* 353-373.
16. Das, A., Raj, B., Mohapatra, M., Andersen, S. M., &Basu, S. (2022). Performance and future directions of transition metal sulfide-based electrode materials towards supercapacitor/ supercapattery. *Wiley Interdisciplinary Reviews: Energy and Environment, 11*(1), e414.
17. Chen, X., Liu, Q., Bai, T., Wang, W., He, F., & Ye, M. (2021). Nickel and cobalt sulfide-based nanostructured materials for electrochemical energy storage devices. *Chemical Engineering Journal, 409*, 127237.
18. Li, Y., Peng, H., Yang, L., Dong, H., & Xiao, P. (2016). Investigating the effect of sulfur and selenium on the electrochemical properties of nickel–cobalt oxides: enhanced charge capacity and composition–property relationships. *Journal of Materials Science, 51,* 7108-7118.
19. Ndambakuwa, W., Ndambakuwa, Y., Choi, J., Fernando, G., Neupane, D., Mishra, S. R., ... & Gupta, R. K. (2021). Nanostructured nickel-cobalt oxide and sulfide for applications in supercapacitors and green energy production using waste water. *Surface and Coatings Technology, 410*, 126933.
20. Zheng, Y., Wang, X., Zhao, W., Cao, X., & Liu, J. (2018). Phytic acid-assisted synthesis of ultrafine NiCo2S4 nanoparticles immobilized on reduced graphene oxide as high-performance electrode for hybrid supercapacitors. *Chemical Engineering Journal, 333*, 603-612.
21. Beka, L. G., Li, X., & Liu, W. (2017). Nickel Cobalt Sulfide core/shell structure on 3D Graphene for supercapacitor application. *Scientific reports, 7*(1), 2105.
22. Zhang, X., Liao, H., Liu, X., Shang, R., Zhou, Y., & Zhou, Y. (2020). Graphitic carbon nitride nanosheets made by different methods as electrode material for supercapacitors. *Ionics, 26*, 3599-3607.
23. Jiang, D., Xu, Q., Meng, S., Xia, C., & Chen, M. (2017). Construction of cobalt sulfide/graphitic carbon nitride hybrid nanosheet composites for high performance supercapacitor electrodes. *Journal of Alloys and Compounds, 706*, 41-47.
24. Ensafi, A. A., Abarghoui, M. M., & Rezaei, B. (2019). Graphitic carbon nitride nanosheets coated with Ni2CoS4 nanoparticles as a high-rate electrode material for supercapacitor application. *Ceramics International, 45*(7), 8518-8524.
25. Ali, S., Raza, M., & Ahmad, A. Facile Synthesis of Zinc Cobalt Sulfide and Composite with Graphitic Carbon Nitride (Zcs@ Gcn) for Photocatalysis and Electrode for Energy Storage Applications. *Available at SSRN 5002268*
26. Zhang, S., Zhao, L., Zeng, M., Li, J., Xu, J., & Wang, X. (2014). Hierarchical nanocomposites of polyaniline nanorods arrays on graphitic carbon nitride sheets with synergistic effect for photocatalysis. *Catalysis Today, 224*, 114-121.
27. Tao, R., Polizos, G., Li, M., Dixit, M., Sharma, J., & Li, J. (2024). Freeze Tape Casting Electrode with Bilayered Architecture for High-Performance Lithium-Ion Batteries. *ACS Applied Energy Materials, 7*(3), 856-861.
28. Goel, A., Mashangva, T. T., Prasher, S., Sharma, A., & Kumar, M. (2024). Facile synthesis and characterization of NiCo2O4-rGO binary for energy-storing application. *Journal of Applied Electrochemistry*, 1-11.
29. S.M. Abdo, S.I. El-Hout, M.N. Rashed, T.I. El-Dosoqy, S.M. El-Sheikh, Boosting visible-light photodegradation of

methyl orange and ibuprofen over rGO-supported Ag3PO4 nanocomposite, Inorg. *Chem. Commun. 161* (2024) 112035.
30. Shakir, I. (2024). Bimetallic CoS-CuCo2O4 composite microstructure decorated on Ni foam as highly efficient electrode material for advanced supercapacitor applications. *Materials Science and Engineering: B, 299*, 116925.
31. Li, X., Zhang, J., Shen, L., Ma, Y., Lei, W., Cui, Q., & Zou, G. (2009). Preparation and characterization of graphitic carbon nitride through pyrolysis of melamine. *Applied Physics A, 94*, 387-392.